Extended Abstracts of the 2019 International Conference on Solid State Devices and Materials, Nagoya, 2019, pp345-346

Oxygen vacancy distribution control for resistive switching of epitaxial TiO_{2-x} thin films in four-terminal memristive devices

Ryotaro Miyake, Zenya Nagata, Tetsuya Tohei and Akira Sakai

Graduate School of Engineering Science, Osaka University
1-3, Machikaneyama-cho, toyonaka-shi
Osaka 560-8531, Japan
Phone : +81-6-6850-6300 E-mail : sakai@ee.es.osaka-u.ac.jp

Abstract

We fabricated epitaxial TiO_{2-x} thin film based four-terminal memristive devices which show much enhanced resistive switching (RS) properties. Origin of RS characteristics and optimized thin-film conditions for enhanced performance were investigated with the aid of microscopic observations and a finite element method simulation model.

1. Introduction

Resistive switching (RS) in memristors is expected to be applied to non-volatile memory devices and neuromorphic computing. One of commonly accepted models of RS phenomenon is formation and rupture of conductive filaments, which are commonly created by the electroforming process, and they often cause a fluctuation of resistance switching phenomena deice-to-device.

In this study, we fabricated four-terminal devices consisting of epitaxial thin films of TiO_{2-x} and evaluated their electrical properties. In our device, two-dimensional variation of oxygen vacancy distribution in TiO_{2-x} plays a key role in realizing the resistive switching. We verified the RS mechanisms based on microscopic observations and a simulation model of dynamic distribution of oxygen vacancies, and clarified the influence of film thickness and resistivity on RS properties.

2. Experimental

Fabrication

Epitaxial thin films of TiO_{2-x} were prepared on non-doped rutile-TiO_2(001) single crystal substrates by pulsed laser deposition (PLD) using a Nd:YAG laser (λ=266 nm). During deposition, substrates were kept at 500 °C and an oxygen gas partial pressure was set at a certain value. Laser fluence was controlled to obtain a growth rate ranging from 2.5 to 3.0 nm/min. We have fabricated TiO_{2-x} epitaxial thin films with different thickness and resistivity. After deposition of the film, four-terminal planer devices were fabricated by sputtering Pt films through the metal mask. The four electrode terminals were respectively labeled as T1 to T4 as shown in Fig. 1(a).

Voltage application protocol

To examine the RS property in the four-terminal device, electrical measurements were performed by applying voltages according to the sequence shown in Fig. 1(b). $R_{1\text{-}3}$ ($R_{2\text{-}4}$), the resistance value between T1 (T2) and T3 (T4) was measured by applying a read voltage of 1 V to T1 (T2) while T3 (T4) was grounded. Subsequently, write voltages $V_{2,4}$ were simultaneously applied to T2 and T4 for t seconds while T1 and T3 were grounded. This cycle was repeated by changing the voltage $V_{2,4}$ from V_M to V_m in 1 V steps (Fig. 1(b)).

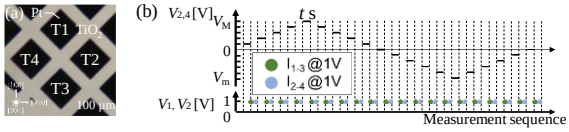

Fig. 1 (a) Optical micrographs showing the four-terminal device. (b) Time series of applied voltage $V_{2,4}$. $I_{1\text{-}3}$ and $I_{2\text{-}4}$ were measured at 1 V between respective steps of $V_{2,4}$ application.

Simulation model

We constructed a two-dimensional (2D) finite element simulation model considering drift and diffusion of n-type dopant (oxygen vacancy), and evaluated the dopant density distribution between terminals. First, carrier density distribution n, p and potential distribution φ are determined by solving the carrier continuity equations (1) and (2) and the Poisson equation (3). Next, we solve the continuity equation (4) in consideration of the drift and diffusion of dopant to obtain a new donor density distribution N_D.

$$\nabla \cdot \left(qp\mu_p \nabla\varphi + qD_p \nabla p\right) = 0 \quad (1)$$

$$\nabla \cdot \left(qn\mu_n \nabla\varphi - qD_n \nabla n\right) = 0 \quad (2)$$

$$\nabla^2 \ \varphi = -\frac{q}{\epsilon}(p - n + N_d - N_a) \quad (3)$$

$$q\frac{dN_d}{dt} = \nabla(qn\mu_i \ \nabla\varphi - qD_i \nabla N_d) \quad (4)$$

We evaluated modulation of donor density distribution under specific voltage application conditions by solving (1)(2)(3) and (4) recursively.

3. Results and discussion

Oxygen vacancy distribution and resistive switching

The sequence of voltage (Fig. 1(b)) was applied to the device consisting of the TiO_{2-x} layer with a thickness of 65 nm and a resistivity of 2.8×10^{-3} Ω cm. V_M and V_m were +8 V and -8 V, respectively, t =100 s, and the cycle was repeated six times. Fig. 2(a) (2(b)) shows variations of $R_{1\text{-}3}$ ($R_{2\text{-}4}$) as a function of applied $V_{2,4}$. We observed that when the $R_{1\text{-}3}$ value decreases the $R_{2\text{-}4}$ value increases, and vice versa. This indicates that the $R_{1\text{-}3}$ and $R_{2\text{-}4}$ variations are complementary to each other. With increasing $V_{2,4}$ value, the sharp decrease (increase) in $R_{1\text{-}3}$ ($R_{2\text{-}4}$), a so-called SET (RESET) operation, occurs at +6 V, so that LRS (HRS) is achieved. After the SET (RESET) operation occurs, with decreasing $V_{2,4}$ value, a sharp increase (decrease) in $R_{1\text{-}3}$ ($R_{2\text{-}4}$) occurs at -6 V, so that HRS (LRS) is achieved. By applying such voltages cyclically, the

resistance can well be tuned repeatedly. The maximum resistance ratio of HRS to LRS was more than 20 in the present thin-film based device (Fig. 2(a)(b)). This is a remarkable improvement compared to our previous devices using thermally reduced rutile TiO_2(001) single crystal substrates, in which the resistance ratio was 2 to 3 [1].

We performed microscopic observations of the device to clarify the RS mechanism during the cyclic application of $V_{2,4}$. The local concentration of oxygen vacancies is well reflected in the color of the TiO_{2-x} crystal, in which a region with a higher (lower) concentration of oxygen vacancy colored (colorless) [1]. Figs. 2(c) and 2(d) show optical micrographs of the device at the stages of $V_{2,4}$ = +8 V and -8 V in the second cycle, respectively. The observed colored (colorless) region between T1 and T3 shown in Fig. 2(c) (2(d)) well reflects the measured lower (higher) resistance between T1 and T3. Thus, we can obtain insights into the microstructural changes of the device which is directly related to the RS phenomena.

Figs. 2(e) and 2(f) show simulation results of oxygen vacancy distribution modified by applying voltage of the same waveform as Fig. 1(b). After applying V_M (V_m), dopant accumulated region, which is colored in light green, is distributed between T1 (T2) and T3 (T4). The simulation results well reproduce the observed distribution of the colored regions shown in Figs. 2(c) and 2(d). Figs. 2(g) and 2(h) are the simulated current density distribution at the read voltage V_{read} application for the respective states of Figs. 2(e) and 2(f). When the dopants are accumulated between T1 (T2) and T3 (T4), the current density between T1 and T3 becomes high (low), which is consistent with the experimentally observed RS. Thus our proposed RS model of 2D oxygen vacancy redistribution is verified by the present experimental and simulation results.

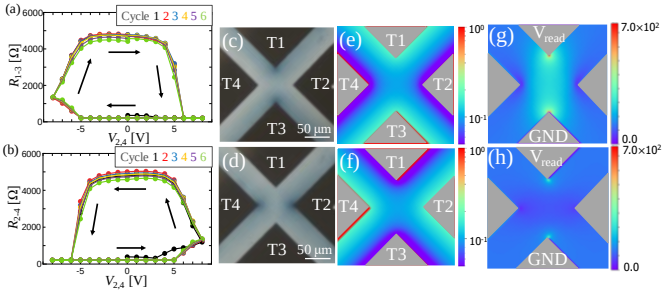

Fig. 2 (a, b) Variation of (a)R_{1-3} and (b)R_{2-4} depending on $V_{2,4}$. (c, d, e, f) (c)(d) Optical micrographs and simulation results of (e)(f) oxygen vacancy distribution and (g)(h) current density distribution, which were obtained at (c)(e)(g) V_M and (d)(f)(h) V_m.

Effect of the layer resistivity and thickness on RS properties

In order to investigate the influence of layer resistivity and thickness of TiO_{2-x} thin films on memristor properties, we fabricated two series of samples with resistivity and thickness as variables. The sequence of voltage (Fig. 1(b)) were applied to the devices where V_M and V_m were adjusted to the most suitable condition for each device, with t =100 s and the cycle was repeated six times. Fig. 3(a) (3(b)) shows the dependence of the ratio R_{off}/R_{on} on the resistivity (thickness) of the TiO_{2-x} layer. The maximum value of R_{off}/R_{on} ratio was obtained for a resistivity of 2.8 × 10^{-3} Ω cm and a thickness of 65 nm (black dotted line). This indicates that there is an optimized resistivity and thickness to obtain a high R_{off}/R_{on} ratio. Fig. 3(c) (3(d)) shows a plot of R_{off} and R_{on} values corresponding to the respective R_{off}/R_{on} ratio versus the film resistivity (thickness). As shown in Fig. 3(c), the observed low R_{off}/R_{on} ratio is found to come from the lower R_{off} (higher R_{on}) value for the resistivity less (more) than 2.8 × 10^{-3} Ω cm. This result is possibly due to the different density of oxygen vacancies. Low (High) resistivity certainly implies high (low) doping levels of oxygen vacancies, making it difficult to create a region with a lower (higher) concentration of oxygen vacancies. On the other hand, in Fig. 3(d), both R_{off} and R_{on} values are reduced as the thickness increases but the reduction ratio of R_{on} is slightly larger (smaller) for the thicknesses less (more) than 65 nm compared with that of R_{off}. To gain insights into this resistance reduction, microscopic observations were performed. Figs. 3(e) and 3(f) depict optical micrographs of devices with two different film thicknesses subjected to six cycles of voltage application sequence. It is found that the device with a thickness of 65 nm had colored regions at the tips of T1 and T3 (surrounded by a red dotted line) while R_{1-3} was in HRS. This type of region is known to be formed by the irreversible accumulation of oxygen vacancies and have low resistance [1], which likely lead to a decrease in the R_{off}.

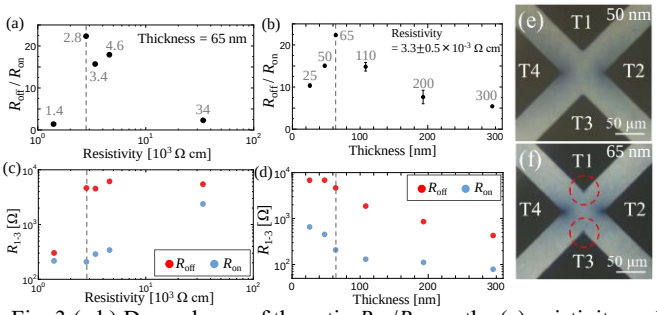

Fig. 3 (a,b) Dependence of the ratio R_{off}/R_{on} on the (a)resistivity and (b)thickness of the TiO_{2-x} layer. (c,d) Dependence of R_{off}, R_{on} on the (c)resistivity and (d)thickness. (e,f) Optical micrographs of the device after applying sequence of voltage for six times. Thickness of layer is (e)50nm, (f)65 nm, respectively.

4. Conclusions

In summary, we investigated RS properties and mechanisms of thin-film-based four-terminal memristive device by experiments and simulations. We also clarified conditions of layer resistivity and thickness for enhanced memristor performance. The present results prove the validity of our proposing RS model involving 2D redistribution of oxygen vacancy between multiple terminals.

Acknowledgements

This work was supported by a KAKENHI Grant-in-Aid (Nos. JP17H03236, and JP17K18881) from the Japan Society for the Promotion of Science (JSPS) and a grant from the Murata Science Foundation.

References

[1] S. Takeuchi *et al.*, Scientific Reports **9**, 2601 (2019)